Journal of Computational Mathematics, Vol.17, No.3, 1999, 327–336.

TWO DIMENSIONAL RIEMANN PROBLEM FOR GAS DYNAMICS SYSTEM IN THREE PIECES*[1)]

Jie-quan Li
(*Institute of Mathematics, Academia Sinica, Beijing 100080, China*)
Shu-li Yang
(*Institute of Applied Mathematics, Academia Sinica, Beijing, 100080, China*)

Abstract

The Riemann problem for two-dimensional flow of polytropic gas with three constant initial data is considered. Under the assumption that each interface of initial data outside of the origin projects exactly one planar wave of shock, rarefaction wave or contact discontinuity, it is proved that only two kinds of combinations, **JRS** and **Js**, are reasonable. Numerical solutions are obtained by using a nonsplitting second order accurate MmB Scheme, and they efficiently reflect the complicated configurations and the geometric structure of solutions of gas dynamics system.

Key words: Two-dimensional Riemann problem, MmB scheme, gas dynamics.

1. Introduction

It is well known that the Riemann problem plays an essential role in developing one-dimensional theory of hyperbolic conservation laws[3] and it is the simplest one of general Cauchy problem and much easier to clarify the explicit structure of its solutions. On the other hand, the solution of the Cauchy problem can be locally approached by the solutions of Riemann problem. Hence the Riemann problem serves as the touchstone and the building block of mathematical theory of hyperbolic conservation laws. Of course, the most interesting and important model is the Euler equations in gas dynamics.

The Riemann Problem for two-dimensional unsteady flow of inviscid, polytropic gas with four piece constant in each quadrant was investigated by Zhang and Zheng in [10], and Chang, Chen and Yang in [2] etc.. With the characteristic analysis and the numerical method, a set of conjecture on the structure of solutions is formulated. Unfortunately, nothing analytic has eventually been solved, although there are still many mathematicians who present various simplified models and try to approach the conjecture and to explain the complicated configurations in gas dynamics system. Therefore it is worthwhile to consider much simpler Riemann initial data in two dimensions.

* Received March 21, 1997.
1) The first author was supported by State Key Laboratory of Scientific and engineering computing, Academia Sinica. The second author was supported by NNSF of China.

The present paper deals in detail with the Riemann problem in three pieces for gas dynamics system, i.e.

$$\begin{cases} \rho_t + (\rho u)_x + (\rho v)_y = 0, \\ (\rho u)_t + (\rho u^2 + p)_x + (\rho uv)_y = 0, \\ (\rho v)_t + (\rho uv)_x + (\rho v^2 + p)_y = 0, \\ \Big(\rho\Big(e + \dfrac{u^2+v^2}{2}\Big)\Big)_t + \Big(\rho u\Big(h + \dfrac{u^2+v^2}{2}\Big)\Big)_x + \Big(\rho v\Big(h + \dfrac{u^2+v^2}{2}\Big)\Big)_y = 0, \end{cases} \tag{1.1}$$

where $\rho, (u, v)$ and p, $e = \dfrac{p}{(\gamma-1)\rho}$, $h = e + \dfrac{p}{\rho}$, $\gamma > 1$ denote density, velocity, pressure, specific internal energy, specific enthalty and polytropic index respectively. And Riemann data in three pieces are described as follows,

$$(\rho, p, u, v)|_{t=0} = T_i, \qquad (i = 1, 2, 3), \tag{1.2}$$

where T_i are constant states (See Fig.1.1), being selected under the assumption (H) that exactly one planar wave of shock, rarefaction wave or contact discontinuity issues from each interface of initial data outside of the origin. It's proved that only two cases, **JRS** and **three Js**, are in theory reasonable. Here we use a nonsplitting second order accurate MmB (locally Maximum-minimum Bounds preserving) scheme to obtain the numerical results for these two cases. MmB schemes are basically derived from the structure of the equation and the solution properties of scalar conservation laws[5], and are generalized to hyperbolic systems. The nonsplitting Mmb schemes have the second order accurate, high resolution and nonoscillatory properties, and have been used to solve many other problems concerning discontinuous solutions fruitfully[6,7].

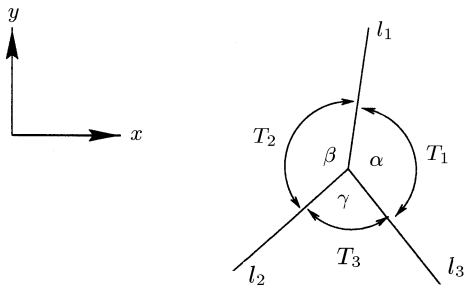

Fig.1.1 Distribution of the initial data

This paper is organized as follows. Section 2 gives the necessary preliminaries. In Section 3 we discuss the distribution of initial data carefully. And the characteristic analyses are presented and the corresponding numerical results are illustrated in Section 4.

2. Preliminaries

In this section we begin by recalling the main results in [2, 10] as our necessary preliminaries.

Noting that the dynamic similarity of (1.1) and lack of characteristic length parameter imply that the solutions be the functions of the variables ξ and η, where $\xi = x/t$, $\eta = y/t$, we seek the self-similar solutions.

$$(\rho, p, u, v) = (\rho, p, u, v)(\xi, \eta). \tag{2.1}$$

The characteristic for (1.1) in (ξ, η)-plane is either

$$\lambda = \lambda_0 = \frac{V}{U}, \quad \text{(pseudoflow characteristic)}, \tag{2.2}$$

or

$$\begin{aligned}\lambda = \lambda_\pm &= \frac{UV \pm \sqrt{c^2(U^2+V^2-c^2)}}{U^2-c^2} \\ &= \frac{V^2-c^2}{UV \mp \sqrt{c^2(U^2+V^2-c^2)}} \quad \text{(pseudowave characteristics)},\end{aligned} \tag{2.3}$$

where $(U, V) = (u - \xi, v - \eta)$ (pseudovelocity) and $c^2 = \gamma p/\rho$ (the sound speed). Due to the well known reasons, it's natural to consider discontinuous solutions. Assume $\eta = \eta(\xi)$ to be the discontinuity line, by Rankine-Hugoniot condition we have then linear(contact) discontinuity

$$\frac{d\eta}{d\xi} = \frac{V}{U} = \frac{V_0}{U_0} = \sigma_0, \tag{2.4}$$

or nonlinear discontinuities,

$$\frac{d\eta}{d\xi} = \frac{U_0V_0 \pm \sqrt{\overline{c}^2(U_0^2+V_0^2-\overline{c}^2)}}{U_0^2-\overline{c}^2} = \sigma_\pm, \tag{2.5}$$

where (ρ, p, u, v) and $(\rho_0, p_, u_0, v_0)$ denote the left and right states along any discontinuity line, and $\overline{c}^2 = \dfrac{p-p_0}{\rho-\rho_0}$.

The system (1.1) must be supersonic at the infinity in (ξ, η)-plane[6], and the infinity can be considered as a Cauchy support. In the neighborhood of the infinity, the solution must consists of planar waves $(\rho, p, u, v)(\mu\xi + \nu\eta)$, which involves:

(i). constant states (ρ_0, p_0, u_0, v_0);

(ii). rarefaction waves (R);

$$R: \begin{cases} u_{t,1} = u_{t,2}, \\ u_{n,1} = u_{n,2} \pm \displaystyle\int_{\rho_2}^{\rho_1} \frac{c}{\rho} d\rho, \\ \rho_1 < \rho_2 \text{ or } \rho_1 > \rho_2, \\ p_1\rho_1^{-\gamma} = p_2\rho_2^{-\gamma}; \end{cases} \tag{2.6}$$

(iii) shock waves (S);

$$S: \begin{cases} u_{t,1} = u_{t,2}, \\ u_{n,1} = u_{n,2} \pm \sqrt{\dfrac{p'_{12}}{\rho_1\rho_2}}(\rho_1 - \rho_2), \\ \dfrac{p_1}{p_2} = \dfrac{(\gamma+1)\rho_1 - (\gamma-1)\rho_2}{(\gamma+1)\rho_2 - (\gamma-1)\rho_1}, \\ \rho_1 > \rho_2 \text{ or } \rho_1 < \rho_2; \end{cases} \tag{2.7}$$

(iv) positive and negative slip lines ($J^{\pm}$)

$$J^{\pm}: \begin{cases} u_{n,1} = u_{n,2}, \\ p_1 = p_2 \\ curl(u_n, u_t)|_J = \pm\infty, \end{cases} \tag{2.8}$$

where u_n and u_t denote the normal and the tangential components of the velocity along any characteristic or discontinuity line, curl $(u, v) = v_x - u_y$, $p'_{12} = \dfrac{p_1 - p_2}{\rho_1 - \rho_2}$.

According to [10], we have conjectures for the general pseudostationary flow that: (1). The pseudostationary is continuous on the whole plane if and only if it is continuous and rarefactive in the neighborhood of infinity; (2). The psedo-stationary flow is smooth (i.e. C^1) on the whole plane if and only if it is a constant state.

3. Analysis of Distribution of Initial Data

In this section, we will discuss the distribution of initial data in detail. At first, we give the classification.

3.1. Classification.

Under the assumption (H), in the neighborhood of infinity, the solution only consists of three planar elementary waves in addition to the constant states. One can easily find that the possible combinations of waves are as follows.

(a). three Rs; (b). three Ss; (c). one S and two Rs, or one R and two Ss; (d). one J and two Rs, or one J and two Ss; (e). one J and one R and one S; (Abbr.**JRS**) (f). three **Js.**

Next, we will show the following theorem holds.

Theorem. *The first four cases are impossible, and only the last two cases are reasonable theoretically.*

Remark. In the experiment that a planar moving incident shock wave encounters a sharp compressive corner [1], regular reflection, Mach reflection etc. are observed. Case (b) shows that in the neighborhood of the triple point, there may exist a slip line besides the incident shock wave, the reflected shock wave and the Mach Stem.

3.2 The proof of the theorem

By the nature of system (1.1), We always think that l_1 coincides with y-axis in the initial plane under a suitable rotation transformation of the coordinate system (cf. Fig.1.1) Next, we will prove the theorem case by case.

Case (a) In this case, we just consider the subcase $\rho_3 < \rho_2 < \rho_1$, and the other subcases are similar.

Obviously, the relations (2.10) hold, i.e.

$$R_{12}: \begin{cases} u_1 - u_2 = \frac{2\sqrt{A\gamma}}{\gamma-1}(\rho_1^{\frac{\gamma-1}{2}} - \rho_2^{\frac{\gamma-1}{2}}), \\ v_1 = v_2, \end{cases} \tag{3.1}$$

$$R_{23}: \begin{cases} u'_2 = u'_3, \\ v'_2 - v'_3 = \frac{2\sqrt{A\gamma}}{\gamma-1}(\rho_2^{\frac{\gamma-1}{2}} - \rho_3^{\frac{\gamma-1}{2}}), \end{cases} \tag{3.2}$$

and

$$R_{31}:\begin{cases} u_1''=u_3'', \\ v_1''-v_3''=\frac{2\sqrt{A\gamma}}{\gamma-1}(\rho_1^{\frac{\gamma-1}{2}}-\rho_3^{\frac{\gamma-1}{2}}), \end{cases} \tag{3.3}$$

where

$$\begin{cases} u'=u\cdot\cos(\beta-\pi/2)+v\cdot\sin(\beta-\pi/2)=u\cdot\sin\beta-v\cdot\cos\beta, \\ v'=-u\cdot\sin(\beta-\pi/2)+v\cdot\cos(\beta-\pi/2)=u\cdot\cos\beta+v\cdot\sin\beta, \end{cases} \tag{3.4}$$

$$\begin{cases} u''=u\cdot\sin\alpha+v\cdot\cos\alpha, \\ v''=-u\cdot\cos\alpha+v\cdot\sin\alpha, \end{cases} \tag{3.5}$$

and A is the entropy.

By (3.1)–(3.3), one can get

$$u_1-u_2=\Big(-\frac{1}{\sin\beta}+\frac{1}{\sin\alpha}\Big)(v_1-v_3), \tag{3.6}$$

and

$$u_1-u_2=-(\cot\alpha+\cot\beta)(v_1-v_3). \tag{3.7}$$

(3.6) and (3.7) show that

$$\sin(\alpha+\beta)=\sin\alpha-\sin\beta,$$

i.e.

$$\sin\alpha=\sin\beta+\sin\gamma. \tag{3.8}$$

Furthermore, we have

$$\sin\beta=\sin\gamma+\sin\alpha, \tag{3.9}$$

$$\sin\gamma=\sin\alpha+\sin\beta. \tag{3.10}$$

(3.8)–(3.10) lead to

$$\sin\alpha=\sin\beta=\sin\gamma=0, \tag{3.11}$$

which means

$$\alpha,\beta,\gamma=0,\quad\text{or}\quad\pi. \tag{3.12}$$

This show that it is impossible that there are only three planar rarefaction waves issuing from the jumps in initial data.

Case (b) By Rankine-Hugoniot condition, we have

$$\begin{cases} \dfrac{p_i}{p_j}=\dfrac{(\gamma+1)\rho_i-(\gamma-1)\rho_j}{(\gamma+1)\rho_j-(\gamma-1)\rho_i}\quad(i,j=1,2,3,i\neq j), \\ p_i\neq p_j, \end{cases} \tag{3.13}$$

which implies that

$$\frac{z-\mu^2}{1-\mu^2 z}=\frac{x-\mu^2}{1-\mu^2 x}\cdot\frac{y-\mu^2}{1-\mu^2 y}, \tag{3.14}$$

where $\mu^2 = \dfrac{\gamma-1}{\gamma+1}$, $x = \dfrac{\rho_1}{\rho_2}$, $y = \dfrac{\rho_2}{\rho_3}$, $z = \dfrac{\rho_1}{\rho_3}$.

Noting that

$$z = xy, \tag{3.15}$$

we obtain that

$$(x-1)(y-1)(z-1) = 0. \tag{3.16}$$

It follows that at least one of x, y and z equals to 1, which contradicts to (3.13).

Case (c) For this case, if suffices to notice the following lemma.

Consider the properties in the phase plane (τ, p), and let

$$\begin{aligned} R(Q_0) &= \{(\tau,p)|p\tau^\gamma = p_0\tau_0^\gamma\}, \\ S(Q_0) &= \{(\tau,p)|\tau(p+\mu^2 p_0) = \tau_0(p_0+\mu^2 p)\}, \end{aligned} \tag{3.17}$$

where $\tau = \dfrac{1}{\rho}$, we have the lemma.

Lemma. (1) $S(Q_0) \cap S(Q_1) = \emptyset$ *if* $Q_1 \in R(Q_0)$. (2) $R(Q_0) \cap R(Q_1) = \emptyset$ *if* $Q_1 \in R(Q_0)$.

The proof of this lemma is trivial and omitted, from which it is easy to know that it is impossible for this case to appear.

Case (d) The two subclasses are similar, we only consider the latter. Without loss of generality, suppose the Riemann data are selected such that the following relations hold,

$$J_{12}: \begin{cases} u_1 = u_2, \\ p_1 = p_2; \end{cases} \tag{3.18}$$

$$S_{23}: \begin{cases} u_2' = u_3', \\ v_2' - v_3' = \sqrt{\dfrac{p_{23}'}{\rho_2\rho_3}}(\rho_2 - \rho_3), \\ \dfrac{p_2}{p_3} = \dfrac{(\gamma+1)\rho_2 - (\gamma-1)\rho_3}{(\gamma+1)\rho_3 - (\gamma-1)\rho_2}, \\ p_2 < p_3, \end{cases} \tag{3.19}$$

and

$$S_{13}: \begin{cases} u_1'' = u_3'', \\ v_1'' - v_3'' = \sqrt{\dfrac{p_{13}'}{\rho_1\rho_3}}(\rho_1 - \rho_3), \\ \dfrac{p_1}{p_3} = \dfrac{(\gamma+1)\rho_1 - (\gamma-1)\rho_3}{(\gamma+1)\rho_3 - (\gamma-1)\rho_1}, \\ p_1 < p_3, \end{cases} \tag{3.20}$$

where (u', v') and (u'', v'') are the same as in (3.4) and (3.5). By Rankine-Hugoniot condition, we obtain

$$\rho_1 = \rho_2. \tag{3.21}$$

From (3.18)–(3.21), it is not difficult to get $\tan\beta = -\tan\alpha$. It follows that

$$\alpha + \beta = \pi. \tag{3.22}$$

Thus the 2-D Riemann problem (1.1)–(1.2) degenerates to the 1-D problem, i.e. there are only one shock issuing from the jumps in initial data. This completes the proof.

4. The Characteristic Analysis and Numerical Results

We will employ the characteristic method to understand the structure of solutions, and evaluate them by comparing with the corresponding numerical results.

a. JRS

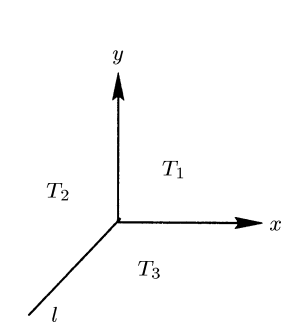

a. Distribution of Initial data

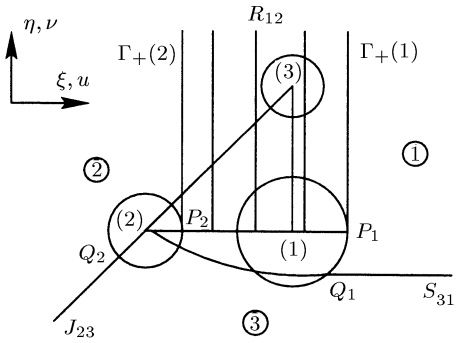

b. Sketch Picture of Solution

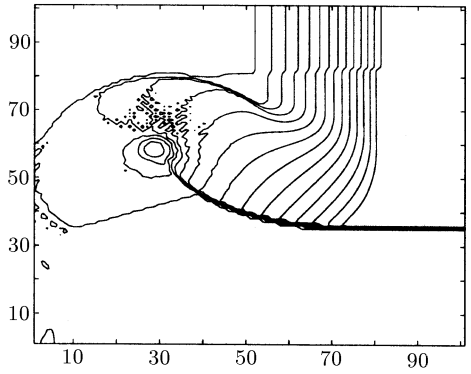

c. Pressure Contour curves

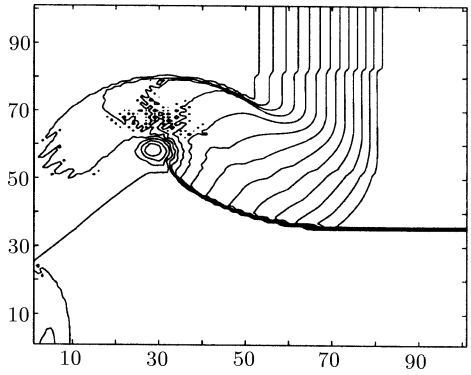

d. Density Contour curves

Fig. 4.1 Mesh points 401×401, Time steps $n = 480$

Through our analysis carefully, it suffices to consider the distribution of Riemann data as shown in Fig.4.1. The relevant compatibility conditions should be

$$R_{12}: \begin{cases} \xi = u_2 + c, \\ u_1 = u_2 + \int_{\rho_1}^{\rho_2} \frac{c}{\rho} d\rho, \\ v_1 = v_2, \\ \frac{p_1}{p_2} = (\frac{\rho_1}{\rho_2})^{\gamma}, \end{cases} \qquad S_{13}: \begin{cases} \eta = \sigma_{13} = u_3 - \sqrt{\frac{\rho_1}{\rho_3} p'_{13}} = u_1 - \sqrt{\frac{\rho_3}{\rho_1} p'_{13}}, \\ u_1 = u_3, \\ v_1 = v_3 - \sqrt{\frac{p_1 - p_3}{\rho_1 \rho_3 (\rho_1 - \rho_3)}} (\rho_1 - \rho_3), \\ \frac{p_1}{p_3} = \frac{(\gamma+1)\rho_1 - (\gamma-1)\rho_3}{(\gamma+1)\rho_3 - (\gamma-1)\rho_1}, \end{cases}$$

and

$$J_{23}: \begin{cases} p_2 = p_3, \\ \frac{u_2 - u_3}{v_2 - v_3} = -\tan\beta. \end{cases}$$

We know that the solution consists of R_{12}, S_{13} and J_{23} besides the three constant states in the neighborhood of infinity in (ξ, η)-plane. Taking the infinity as a Cauchy support and extending the solution along characteristic lines or stream lines, we obtain that R_{12} must meet the sonic stem P_1P_2 and S_{13} can arrive at the sonic circle of the state T_1 at Q_1 before they meet R_{12} since $\sigma_{13} < u_1$, and that J_{23} reach the sonic circle of T_2 at Q_2. Across the circle of T_1, the flow is subsonic and S_{13}, which cuts the constant states T_3 from a subsonic region and form a free-boundary value problem, should match smoothly. From the numerical results, we find it becomes weaker and weaker (See Fig.4.1).

The distribution of initial data is as follows,

$$\begin{array}{llll} u_1 = 0 & v_1 = 0 & \rho_1 = 1 & p_1 = 50 \\ u_2 = -6.86099 & v_2 = 0 & \rho_2 = 0.408327 & p_2 = 14.2686 \\ u_3 = 0 & v_3 = 6.86099 & \rho_3 = 0.431515 & p_3 = 14.2686 \end{array}$$

and $\lambda = \dfrac{\Delta t}{\Delta x} = \dfrac{\Delta t}{\Delta y} = 0.05$

b. Three Js

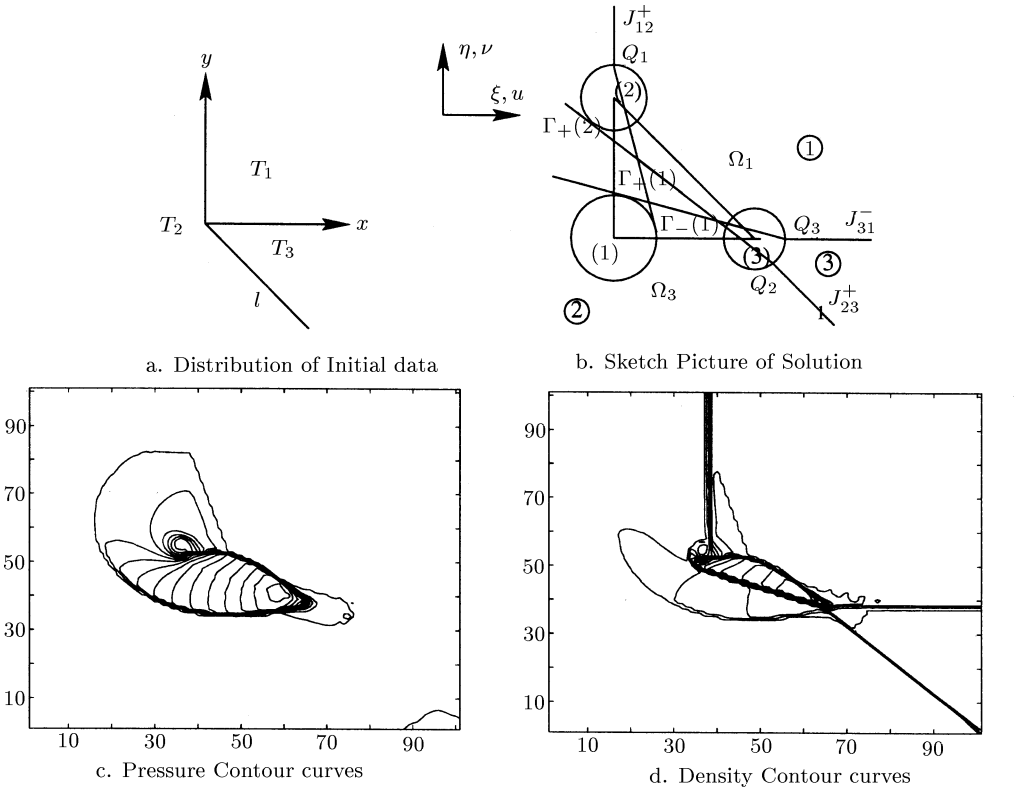

Fig.4.2 Mesh points 401×401, Time steps $n = 420$

In this case, the pressure p is constant. Due to the difference of J^- and J^+, this case is classified as two kinds of subcases.

Subcase 1. $2J^+ + J^-$ The three jumps, J_{12}^+, J_{23}^+ and J_{13}^-, from infinity meet the sonic circles of states T_2 and T_3 at Q_1, Q_2 and Q_3 firstly. We draw the characteristic

lines $\Gamma_+(1), \Gamma_+(2)$ and $\Gamma_-(1)$ through Q_1, Q_2 and Q_3, respectively. It's easy to see that the determination region Ω_1 of T_1 is encompassed by $J_{12}^+, J_{13}^-, \Gamma_+(1)$ and $\Gamma_-(1)$, while $J_{23}, \Gamma_-(3)$, the part of the sonic circle of (1) Q_3Q_4 and J_{13} bound the determined region Ω_3 of the state T_3. Obviously, Ω_1 and Ω_3 may overlap. According to the characteristic theory, there will appear a discontinuous solution which consists of shock waves or/and contact discontinuities. From the numerical results, we observe that J_{12} and J_{23} may interact each other and produce two shock waves, which bound the pseudo-subsonic region, and a contact discontinuity or other new nonlinear waves which have not been testified yet in this region (See Fig.4.2).

The distribution of initial data is as follows,

$u_1 = -1$	$v_1 = -1$	$\rho_1 = 1.5$	$p_1 = 1$
$u_2 = -1$	$v_2 = 1$	$\rho_2 = 0.5$	$p_2 = 1$
$u_3 = 1$	$v_3 = -1$	$\rho_3 = 1$	$p_3 = 1$

and $\lambda = \frac{\Delta t}{\Delta x} = \frac{\Delta t}{\Delta y} = 0.1$

Subcase 2. $3J^-s$. This subcase is similar to the 4Js discussed in [6], our necessary and significant supplement is that a spiral may appear, which is the result of the interaction of Js (see Fig.4.3).

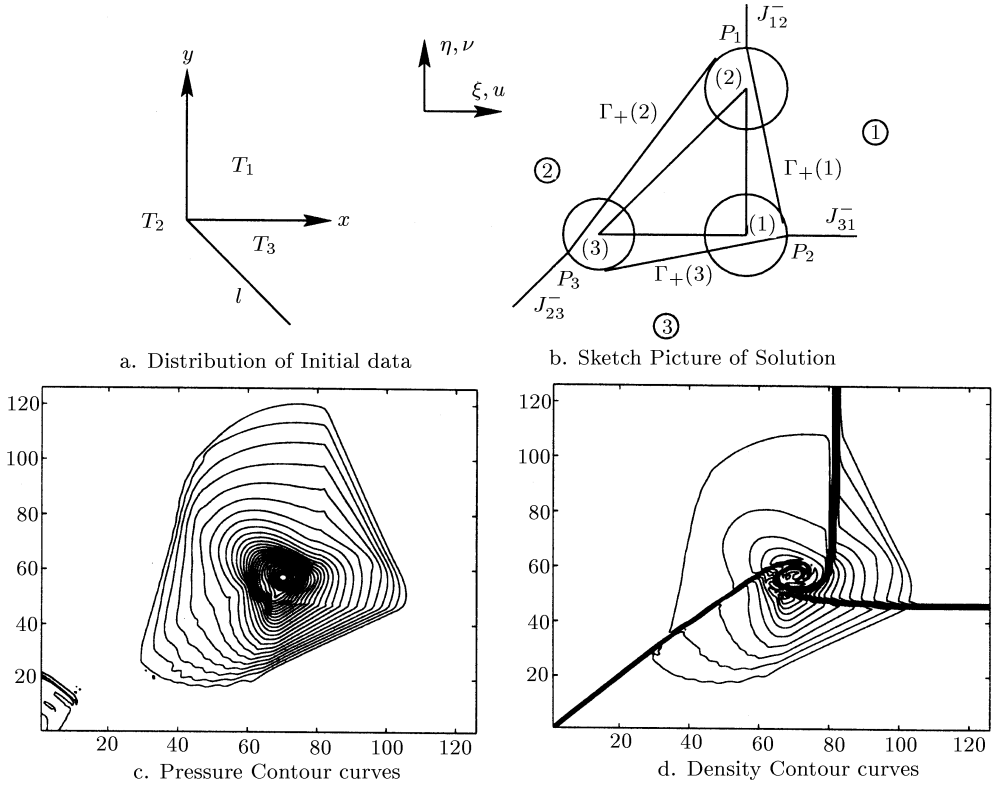

a. Distribution of Initial data

b. Sketch Picture of Solution

c. Pressure Contour curves

d. Density Contour curves

Fig.4.3 Mesh points 401×401, Time steps $n = 360$

The table of initial data is as follows,

$u_1 = 1$	$v_1 = -1$	$\rho_1 = 1.5$	$p_1 = 2$
$u_2 = 1$	$v_2 = 1$	$\rho_2 = 0.5$	$p_2 = 2$
$u_3 = -1$	$v_3 = -1$	$\rho_3 = 1$	$p_3 = 2$

and $\lambda = \dfrac{\Delta t}{\Delta x} = \dfrac{\Delta t}{\Delta y} = 0.2.$

5. Conclusion

From the above analyses and numerical results, we know that Riemann problem are the simplest in 2-D gas dynamics, the structure of solutions is the basis for the study of phenomena appearing in gas dynamics. Furthermore, we find many interesting phenomena similar to those of Riemann problem in multipieces, such as spiral, and the interaction of S and R etc.. Especially, the interaction of J^+ and J^- may produce a new kind of a shock, which we call a delta wave of the solutions[9]. Now we keep on doing both numerical experiments and theoretical proof to check it.

In addition, we find the numerical results are in accordance to the theoretical analyses, which shows that MmB schemes are dependable once again.

Acknowledgement. The authors would like to thank Prof. T. Zhang for his encouragement and careful discussions.

References

[1] Ben-dor. G. and Glass, II, Domains and boundaries of non-stationary oblique shock wave reflection (1), (2), *J. Fluid Mech.,* **92** (1979), 459–96; **96** (1980), 735–56.

[2] T. Chang, G.Q. Chen, S. Yang, On the Riemann Problem for 2-D Compressible Euler Equations, *Discrete and Continuous Dynamical Systems,* **1** : 4 (1995), 555–584.

[3] R. Courant, K. Friedrichs, Supersonic Flow and Shock waves, Interscience, New York, 1948.

[4] T. Chang, L. Hsiao, The Riemann Problem and Interaction of Waves in Gas Dynamics, Longman Scientific and Technical (Pitman Monographs and Surveys in Pure and Applied Mathematics, No.41), Essex, 1989.

[5] Shuli Yang, Calculations of Riemann problem for 2-D scalar conservation laws by second order accurate MmB scheme, *J. of Comp. Math.,***12** : 4 (1994), 339–351.

6] Shuli Yang, Characteristic Petrov-Galerkin schemes for 2-D conservation laws, *IMPCT of Computing in Science and Engineering,* **5** (1993), 379–406.

[7] Shuli Yang, Spirals for Riemann problems in Multipieces for 2-D Euler equations by using MmB schemes, *Proc. of International Conference on Nonlinear Partial Diff. Equat.,* Beijing, June 1993.

[8] Shuli Yang, Tong Zhang, The Mmb difference solutions of 2-D Riemann problems for a 2×2 hyperbolic system of conservation laws, *IMPACT of Comp. Science Engin.,* **3** (1991), 146–180.

[9] T. Chung (T. Zhang), Shuli Yang, Delta Waves in Solutions of Conservation Laws, Proc. of International Conference on Nonlinear Partial Diff. Equat., Beijing, June 1993.

[10] T. Zhang, Y.Zheng, Conjecture on the structure of solutions of the Riemann problem for two-dimensional gas dynamics systems, *SIAM J. Math. Anal.,* **21** (1990), 593–630.